

# Fractal image coding as projections onto convex sets

Mehran Ebrahimi and Edward R. Vrscay

Department of Applied Mathematics  
Faculty of Mathematics  
University of Waterloo  
Waterloo, Ontario, Canada N2L 3G1  
m2ebrahi@uwaterloo.ca, ervrscay@uwaterloo.ca

**Abstract.** We show how fractal image coding can be viewed and generalized in terms of the method of projections onto convex sets (POCS). In this approach, the fractal code defines a set of spatial domain similarity constraints. We also show how such a reformulation in terms of POCS allows additional constraints to be imposed during fractal image decoding. Two applications are presented: image construction with an incomplete fractal code and image denoising.

## 1 Introduction

In this paper we show how fractal image coding can be formulated in terms of a powerful method known as projections onto convex sets (POCS) [15].

In standard fractal image coding [1, 3, 7, 11], images are normally considered as elements of a complete function space  $\mathcal{F}$ , e.g.,  $L^p(X)$ , for  $X \subset \mathbb{R}^2$ . Given an image function  $u$ , we seek a contractive operator  $T : \mathcal{F} \rightarrow \mathcal{F}$  such that its fixed point  $\bar{u}$  is a good approximation to  $u$ . This comprises *fractal coding*. At the *decoding* stage, the *fractal transform*  $T$  is applied iteratively to an initial “seed” image  $u_0$ . Banach’s contraction mapping theorem guarantees the convergence of the iterates defined by  $u_{n+1} = Tu_n$  to  $\bar{u}$ .

One may, however, consider this decoding process to be too restrictive since any additional knowledge about the original image (e.g., bounding constraints on the pixel values) cannot be applied simultaneously with the fractal transform. In practice, therefore, additional constraints have usually been applied to the fixed point of the contraction map  $T$ . Such post-processing is usually equivalent to the application of projections on the fixed point. For example, thresholding the data in order to enforce certain bounds is simply a projection of the the data onto the space of images that lie within those bounds.

In our POCS approach, a fractal code is considered as a set of similarity constraints in the spatial domain. Fortunately these constraints are convex and closed, and therefore satisfy the requirements in setting up a POCS approach.

In what follows, we shall show how POCS can provide the opportunity to apply the fractal code of an image simultaneously with additional constraints

during the decoding stage. These constraints may include other spatial, statistical, spectral and pattern properties of the unknown image, e.g., bounds on pixel values, bounded energy, smoothness, similarity to the observed data, etc..

A most interesting consequence of such a POCS-type reformulation allows us to bypass the traditional view of fractal coding as simply a mapping of domain image subblocks onto range image subblocks. Instead, we consider the application of the projections on a closed and convex set that is constructed using the similarity constraint between the domain and range subblocks. This type of projection translates to a *simultaneous* alteration of domain-range block pairs. In this paper, we introduce such projections explicitly and examine some interesting implications and applications.

Let us qualify that we are not interested in the compression capabilities of fractal image coding here. Our study picks up upon the thesis of H. Puh on set-theoretic coding [13]. In that work, there were no explicit details on how the self-similarity properties of an image can be translated into POCS-type inequality constraints.

## 2 Some basics of fractal image coding

More details on fractal image coding can be found in many places [1, 3, 7, 11], including one of our recent papers on fractal-based denoising [9].

### 2.1 Fractal image encoding

Fractal image coding seeks to approximate an image by a union of spatially-contracted and greyscale-modified copies of subblocks of itself. If we let the image of interest  $I$  be represented by an image function  $u(x, y)$ , then the result of the coding procedure is a contractive mapping  $T$ , the so-called *fractal transform* operator, the fixed point  $\bar{u}$  of which provides an approximation to  $u$ . In other words,

$$u \cong \bar{u} = T\bar{u}. \quad (1)$$

To obtain  $T$ , the image  $I$  is first partitioned (e.g., uniform, quadtree) into a set of nonoverlapping range blocks  $R_i$ . For each range block  $R_i$ , one searches for a larger domain block  $D_i$  (from an appropriate “domain pool”  $\mathcal{D}$  that is often common to all range blocks of the same size) such that  $u(R_i)$  is approximated as well as possible by a modified copy of  $u(D_i)$ , i.e.,

$$u(R_i) \cong \phi_i(u(D_i)) = \phi_i(u(w_i^{-1}(R_i))), \quad (2)$$

where  $\phi_i : \mathbf{R} \rightarrow \mathbf{R}$  is a greyscale map that operates on pixel intensities and  $w_i$  denotes the 1-1 contraction/decimation that maps pixels of  $D_i$  onto pixels of  $R_i$ . The *fractal code* defining  $T$  consists of the maps  $\phi_i$  as well as the domain-range assignments determined during the coding procedure.

In the calculations reported below, we employ the simplest form of partitioning, namely a uniform scheme. The range blocks  $R_i$  will be  $N \times N$  square

nonoverlapping pixel blocks. They will share a common domain pool  $\mathcal{D}$  that consists of all nonoverlapping  $2N \times 2N$  pixel blocks. This choice of domain pool is, of course, nonoptimal. The set of all  $2N \times 2N$  pixel blocks obtained by single pixel-shifts would be better but search times would be enormous. In any case, the purpose of this paper is to show the basics of a method that can be adapted to any partitioning scheme.

Finally, there are 8 ways – four rotations and four inversions – by which a larger square domain block  $D_j$  can be contracted/decimated and then mapped onto a smaller range block  $R_i$ . We shall index these possible transformations by means of a  $k$  superscript in the spatial mapping, i.e.,  $w_i^{(k)} : D_i \rightarrow R_i$ ,  $k = 1, 2, \dots, 8$ .

Let us now assume that we have fractally coded an image function  $u$  according to Eq (2). Because of the nonoverlapping nature of the partition, we may write

$$u(x, y) \cong (Tu)(x, y) = \sum_i \phi_i(u(w_i^{-1}(x, y))). \quad (3)$$

The image function  $u$  is thus approximated as a union of spatially-contracted ( $w_i$ ) and greyscale-distorted ( $\phi_i$ ) copies of itself. This union of modified copies (a trivial consequence since the copies do not overlap) defines a special kind of *fractal transform* operator  $T$ . If the above approximation is a good one, then the so-called *collage distance*  $\|u - Tu\|$  is small. From the ‘‘Collage Theorem’’ [2],

$$\|u - \bar{u}\| \leq \frac{1}{1 - c_T} \|u - Tu\|, \quad (4)$$

it then follows that if  $u$  is ‘‘close’’ to  $Tu$ , then  $u$  is also close to  $\bar{u}$ , the fixed point of  $T$ . Here,  $c_T \in [0, 1)$  denotes the contraction factor of  $T$ . The quantity  $\|u - \bar{u}\|$  is the error of approximation of  $u$  by  $\bar{u}$ .

In practice, one normally assumes the greyscale maps  $\phi_i$  to be affine, i.e.,

$$\phi_i(t) = \alpha_i t + \beta_i. \quad (5)$$

For a given domain-range block pair  $D_j/R_i$ , the optimal value of the  $\alpha$  and  $\beta$  parameters is usually accomplished by means of least-squares fitting. If we let  $x_m$  and  $y_m$ ,  $m = 1, 2, \dots, N^2$  denote the pixel greyscale values of the  $w^{(k)}$ -decimated domain block  $D_j$  and range block  $R_i$ , respectively, then  $\alpha$  and  $\beta$  are determined so that that the squared  $L^2$  ‘‘collage distance’’ over  $R_j$ ,

$$\Delta^{(k)} = \sum_{m=1}^{N^2} [y_m - \alpha x_m - \beta]^2, \quad (6)$$

is minimized. In the construction of the fractal transform operator  $T$ , we choose, for each range block  $R_i$ , the domain block  $D_j \in \mathcal{D}$  and geometric transformation  $w^{(k)}$  which yield the minimum collage distance  $\Delta^{(k)}$ . In this way, the total collage distance  $\|u - Tu\|$  in Eq. (4) is minimized.

## 2.2 Fractal image decoding

Given a contractive fractal transform  $T$ , we may generate its fixed point  $\bar{u}$  by the iteration procedure  $u_{n+1} = Tu_n$ , starting with an arbitrary “seed” image  $u_0$ .



**Fig. 1.** The fractal transform operator designed to approximate the  $256 \times 256$  (8 bpp) “Lena” image (Left). The “seed” image was  $u_0(x) = 255$  (plain white). The fractal transform  $T$  was obtained by “collage coding”  $8 \times 8$  nonoverlapping pixel range blocks. The domain pool was comprised of nonoverlapping  $16 \times 16$  pixel blocks.

In the decoding procedure, the image subblocks  $u_n(R_i)$  of  $u_n$  are replaced by modified copies  $\phi_i(u_n(D_i))$  according to Eq. (2). Banach’s contraction mapping theorem guarantees that the sequence of images  $u_n$  converges to  $\bar{u}$ .

In this scheme, the range blocks  $R_{n+1,i}$  comprising image  $u_{n+1}$  are simply modified versions of appropriate domain blocks  $D_{n,i}$  of  $u_n$ . More precisely,  $u_{n+1}(R_i) = \phi_i(w_i^{(k)}(u_n(D_i)))$ .

In Figure 1 is presented the fixed point approximation  $\bar{u}$  to the standard  $256 \times 256$  Lena image (8 bits/pixel) using a partition of  $8 \times 8$  nonoverlapping pixel blocks ( $64^2 = 4096$  in total). The domain pool for each range block was the set of  $32^2 = 1024$ ,  $16 \times 16$  non-overlapping pixel blocks. (This is clearly not optimal.) This image was obtained by starting with the seed image  $u_0(x) = 255$  (plain white image) and iterating  $u_{n+1} = Tu_n$  to  $n = 15$ .

## 3 Set Theoretic Image Coding and Restoration

The method of projections onto convex sets (POCS) has attracted much attention in a multitude of image restoration and reconstruction applications. The

main reasons are the simplicity, flexibility, and powerful inclusion of *a priori* information. It is generally simple to define convex constraint sets which incorporate desired solution characteristics. These sets may impose restrictions such as positivity or bounded energy which are difficult to represent in terms of cost functionals. The only potential source of difficulty in applying POCS is to determine the projection operators. If the the convex and closed sets are constructed and the projections are found, a point in the intersection these sets can be found if the intersection is not empty.

Assume that  $x$  is known to lie in  $m$  given sets  $C_i$ ,  $i = 1, 2, \dots, m$  where each of the sets represents a constraint on the image. If the sets  $C_i$  are closed and convex, we associate projection operators  $P_i$ ,  $i = 1, 2, \dots, m$ , to each  $C_i$ . The projection of  $h$  onto  $C_i$  is defined as  $g = P_i h$ , with  $g \in C_i$  and

$$\|g - h\| = \inf_{y \in C_i} \|y - h\|. \quad (7)$$

Bregman [4] proved that if the sets  $C_i$ ,  $i = 1, 2, \dots, m$  are closed and convex and  $\bigcap_i C_i \neq \emptyset$ , then the sequence  $\{X^{(n)}\}$  defined recursively as

$$X^{(n+1)} = P_m \dots P_2 P_1 X^{(n)}, \quad (8)$$

converges to a fixed point in the intersection of all  $C_i$ s. In other words,  $X^{(n)}$  converges to a point  $X$ , where  $X \in \bigcap_i C_i$ . This sequence of projections is applied repeatedly to yield an updated estimate of the image. It is imperative to note that the point  $X$  is, in general, nonunique. Its only distinguishing feature is that it lies on the intersection of all constraint sets. In general, it will be dependent on the initial guess  $X^{(0)}$ . Detailed theoretical discussions of the POCS method can be found in [4, 10, 15].

## 4 POCS and fractal image coding

In this section we consider a number of self-similarity constraints along scales which can then be used to reformulate fractal image coding as a POCS method. It is assumed that an image has a continuous representation as a function in  $L^p(X)$  where  $X \subset \mathbf{R}^2$ . The theoretical basis for this discussion (e.g., proofs of propositions) has been presented elsewhere [6].

### 4.1 Self-similarity constraints using collage distances

The collage distance is an important measure of self-similarity. We shall consider three different types of collage distances from which similarity constraints can be built. These are (i) the total collage distance, (ii) the collage distance for a fixed domain-range block pair and (iii) the pointwise collage distance.

**Definition 1.** For a given image  $u \in L^p(X)$ , where  $1 \leq p \leq \infty$  we introduce the following collage distance definitions.

a) The total collage distance is defined as

$$\begin{aligned}\Delta(u) &= \left\| (Tu) - u \right\|_p \\ &= \left( \int_{(x,y) \in X} \left| \sum_i \phi_i(u(w_i^{-1}(x,y))) - u(x,y) \right|^p dx dy \right)^{\frac{1}{p}},\end{aligned}\quad (9)$$

when  $1 < p < \infty$ . Appropriate definitions are used for  $p = 1$  and  $p = \infty$ .

b) The collage distance for a fixed pair of domain and range blocks is

$$\begin{aligned}\Delta_{(i,j)}^{(k)}(u) &= \left\| \phi_i \left( u(w_{i,j,(k)}^{-1}(R_i)) \right) - u(R_i) \right\|_p \\ &= \left( \int_{(x,y) \in R_i} \left| \phi_i(u(w_i^{-1}(x,y))) - u(x,y) \right|^p dx dy \right)^{\frac{1}{p}},\end{aligned}\quad (10)$$

where  $1 < p < \infty$ . Again, appropriate definitions are used for  $p = 1$  and  $p = \infty$ . As before  $R_i$  is a range block.  $w_{i,j,(k)}^{-1}$ , is the inverse of contraction from  $D_j$  to  $R_i$  and  $(k) = K_{(i,j)} \in \{0, \dots, 7\}$ .

c) The pointwise collage distance is defined as

$$\Delta_{(i,j)(x,y)}^{(k)}(u) = \left| \phi \left( u(w_{i,j,(k)}^{-1}(x,y)) \right) - u(x,y) \right|, \quad (11)$$

where  $(x,y) \in R_i$ .

By its nature, fractal image coding implies perfect self-similarity between elements in the range and domain pool of an attractor image  $\bar{u}$ . In natural images, however, perfect self-similarity generally does not hold. Therefore, a model that is more consistent with the physical world would allow collage distances, as measures of similarity, to deviate from zero but not beyond some threshold value, say  $\delta > 0$ . Such threshold values can be determined based on the application. Such a framework provides more flexibility to incorporate additional knowledge about the image and to relax the perfect self-similarity constraint in order to obtain a better approximation of an image in the reconstruction process. In the perfect self-similarity assumption case, this threshold may be set to zero, representing perfect consistency with traditional fractal image coding.

Each of the three collage distances described above may be used in the procedure. Associated with each collage distance are the following self-similarity constraints in  $L^p(X)$  for  $1 \leq p \leq \infty$ . (i) Based on the total collage distance define

$$\Psi = \left\{ u \in L^p(X) : \Delta(u) \leq \delta \right\}. \quad (12)$$

(ii) Based on range based collage distance define

$$\Psi_{(i,j)}^{(k)} = \left\{ u \in L^p(X) : \Delta_{(i,j)}^{(k)}(u) \leq \delta_{(i,j)}^{(k)} \right\}. \quad (13)$$

(iii) Finally define the set  $\Psi_{(i,j)(x,y)}^{(k)}$  based on the pointwise collage distance as

$$\Psi_{(i,j)(x,y)}^{(k)} = \left\{ u \in L^p(X) : \Delta_{(i,j)(x,y)}^{(k)}(u) \leq \delta_{(i,j)(x,y)}^{(k)} \right\}. \quad (14)$$

Closedness and convexity of these sets can be verified easily under some trivial assumptions [6]. In practice, when dealing with digital images we need to construct new convex and closed sets based on the image greyvalues at discrete points. In the following section, we study the discrete counterpart of  $\Psi_{(i,j)(x,y)}^{(k)}$ .

## 4.2 Discrete pointwise collage constraints and associated projections

When we are working with discrete digital images, we may assume any digital image  $U \in l^2(X)$ , where  $X$  is a bounded subset of  $\mathbf{Z}^2$ . Note that in the continuous case, we considered the set  $\Psi_{(i,j)(x,y)}^{(k)}$  for  $(x, y) \in R_i$ . In the same fashion, for the discrete case, we define  $\Psi_{(i,j)(m,n)}^{(k)}$ , where  $(m, n)$  is a point with integer coordinates over a fixed  $R_i$ .

$$\begin{aligned} \Psi_{(i,j)(m,n)}^{(k)} &= \left\{ U \in l^2(X) : \Delta_{(i,j)(m,n)}^{(k)}(U) \leq \delta_{(i,j)(x,y)}^{(k)} \right\} \\ &= \left\{ U \in l^2(X) : \left| \phi \left( U(w_{i,j,(k)}^{-1}(m, n)) \right) - U(m, n) \right| \leq \delta_{(i,j)(m,n)}^{(k)} \right\} \end{aligned} \quad (15)$$

In the discrete case  $(m, n)$  corresponds to four points  $(s, t)$ ,  $(s, t+1)$ ,  $(s+1, t)$ , and  $(s+1, t+1)$  under the inverse mapping  $w_{i,j,(k)}^{-1}(m, n)$ . Here  $U(w_{i,j,(k)}^{-1}(m, n))$  can be written as

$$U(w_{i,j,(k)}^{-1}(m, n)) = \frac{1}{4} \left\{ U(s, t) + U(s, t+1) + U(s+1, t) + U(s+1, t+1) \right\}. \quad (16)$$

Hence, replacing  $\phi(t) = \alpha t + \beta$  yields

$$\begin{aligned} \Psi_{(i,j)(m,n)}^{(k)} &= \left\{ U \in l^2(X) : \left| \frac{\alpha}{4} \{ U(s, t) + U(s, t+1) + U(s+1, t) \right. \right. \\ &\quad \left. \left. + U(s+1, t+1) \right\} + \beta - U(m, n) \right| \leq \delta_{(i,j)(m,n)}^{(k)} \right\}. \end{aligned} \quad (17)$$

**Proposition 1.** [6]  $\Psi_{(i,j)(m,n)}^{(k)}$  is a closed and convex set on the Hilbert space  $l^2(X)$  provided that  $\phi(t) = \alpha t + \beta$ .

Now that the convex and closed constraints are constructed we have to find the projection operators on these sets.

**Proposition 2.** [6] Assume an element  $U$  is given in the Hilbert space  $l^2(X)$ , where  $X$  is a bounded subset of  $\mathbf{Z}^2$ . Let  $V$  be the projection of  $U$  on  $\Psi_{(i,j)(m,n)}^{(k)}$ .

This projection can be computed in the following manner. Assume that the four points in the set

$$\mathcal{A} = \left\{ (s, t), (s, t + 1), (s + 1, t), (s + 1, t + 1) \right\} \quad (18)$$

are those that are mapped to  $(m, n)$  under the contraction  $w_{i,j,(k)}$ . Set  $\delta = \delta_{(i,j)(m,n)}^{(k)} \geq 0$  and

$$r = \frac{\alpha}{4} \left[ U(s, t) + U(s, t + 1) + U(s + 1, t) + U(s + 1, t + 1) \right] + \beta - U(m, n). \quad (19)$$

In the case that  $(m, n) \notin \mathcal{A}$ , the values  $V(p, q)$  for  $p, q \in \mathbf{Z}$  can be computed as

$$U(p, q) + \begin{cases} \text{Case } (p, q) \in \mathcal{A} \\ \frac{-\alpha/4}{1+4(\alpha/4)^2}(r - \delta), r > \delta \\ 0, |r| \leq \delta \\ \frac{-\alpha/4}{1+4(\alpha/4)^2}(r + \delta), r < -\delta \\ \\ \text{Case } (p, q) = (m, n) \\ \frac{1}{1+4(\alpha/4)^2}(r - \delta), r > \delta \\ 0, |r| \leq \delta \\ \frac{1}{1+4(\alpha/4)^2}(r + \delta), r < -\delta \\ \\ \text{Case } (p, q) \notin \mathcal{A} \cup \{(m, n)\} \\ 0. \end{cases} \quad (20)$$

In the case that  $(m, n) \in \mathcal{A}$ , the values  $V(p, q)$  for  $p, q \in \mathbf{Z}$  can be computed as

$$U(p, q) + \begin{cases} \text{Case } (p, q) \in \mathcal{A} \setminus \{(m, n)\} \\ \frac{-\alpha/4}{(1-\alpha/4)^2+3(\alpha/4)^2}(r - \delta), r > \delta \\ 0, |r| \leq \delta \\ \frac{-\alpha/4}{(1-\alpha/4)^2+3(\alpha/4)^2}(r + \delta), r < -\delta \\ \\ \text{Case } (p, q) = (m, n) \\ \frac{1-\alpha/4}{(1-\alpha/4)^2+3(\alpha/4)^2}(r - \delta), r > \delta \\ 0, |r| \leq \delta \\ \frac{1-\alpha/4}{(1-\alpha/4)^2+3(\alpha/4)^2}(r + \delta), r < -\delta \\ \\ \text{Case } (p, q) \notin \mathcal{A} \\ 0. \end{cases} \quad (21)$$



The above projection can be found using KKT conditions for solving constrained optimization problems. Another approach to prove this proposition is to view the optimization problem as a deblurring of a signal in presence of spatially-varying blur [14]. Now that the constraints  $\Psi_{(i,j)(m,n)}^{(k)}$  and its associated projections are in hand we may apply these constraints in a POCS sequence along with other consistent constraints at the decoding stage.

## 5 Applications

### 5.1 Restoration of an image with an incomplete fractal code

Assume that we are given an incomplete fractal code of an image, i.e., some of the domain-range block assignments and corresponding greyscale map coefficients are missing. In such a case, the usual fractal decoding scheme, in which an arbitrary “seed” image is employed, will collapse since the range blocks of the image for which the fractal code is missing cannot be modified. These blocks will simply remain identical to the corresponding subblocks of the seed image.

To illustrate, let us consider the fractal code associated with the Lena image in Figure 1. Suppose that the fractal code corresponding to all range blocks in the bottom half of the image are missing. Using a random image as the seed, the limiting image produced by the fractal decoding procedure is shown in Figure 2(b). Only the domain blocks in the top-half of the image have been modified – those in the lower half are identical to their counterparts in the seed image. Likewise, if the fractal code is missing for the range blocks depicted in black in Figure 2(d), then fractal coding produces the limiting image in Figure 2(e). We now show how these two situations can be improved using POCS.

The incomplete fractal code problem is an underdetermined, hence ill-posed, inverse problem. There are many possible solutions. We now consider a POCS-type method that will employ the pointwise collage constraints  $\Psi_{(i,j)(m,n)}^{(k)}$  with  $\delta = 0$ , associated with the partially known fractal code. For the problem associated with Figure 2(b), where the fractal code for the bottom half of image is missing, we obtain Figure 2(c) with this POCS method, having once again started with the random seed image. Figure 2(c) is seen to represent a significant improvement over Figure 2(b).

Along with the collage constraints, however, we can impose additional constraints as desired. For example, consider the missing fractal code problem of Figure 2(d). Standard fractal decoding yields Figure 2(e). The POCS method with an additional smoothness constraint produces Figure 2(f), a significant improvement over Figure 2(e). The smoothness constraint was imposed by means of a low-pass filtering operation in the frequency domain.

Let us now explain why the POCS method can yield better approximations to the original image in the case of missing fractal codes, with particular reference to Figures 2(b) and 2(c). As mentioned above, the usual fractal decoding iteration scheme of mapping domain blocks to range blocks does not change the range blocks for which the fractal code is missing, e.g., the bottom part of the image

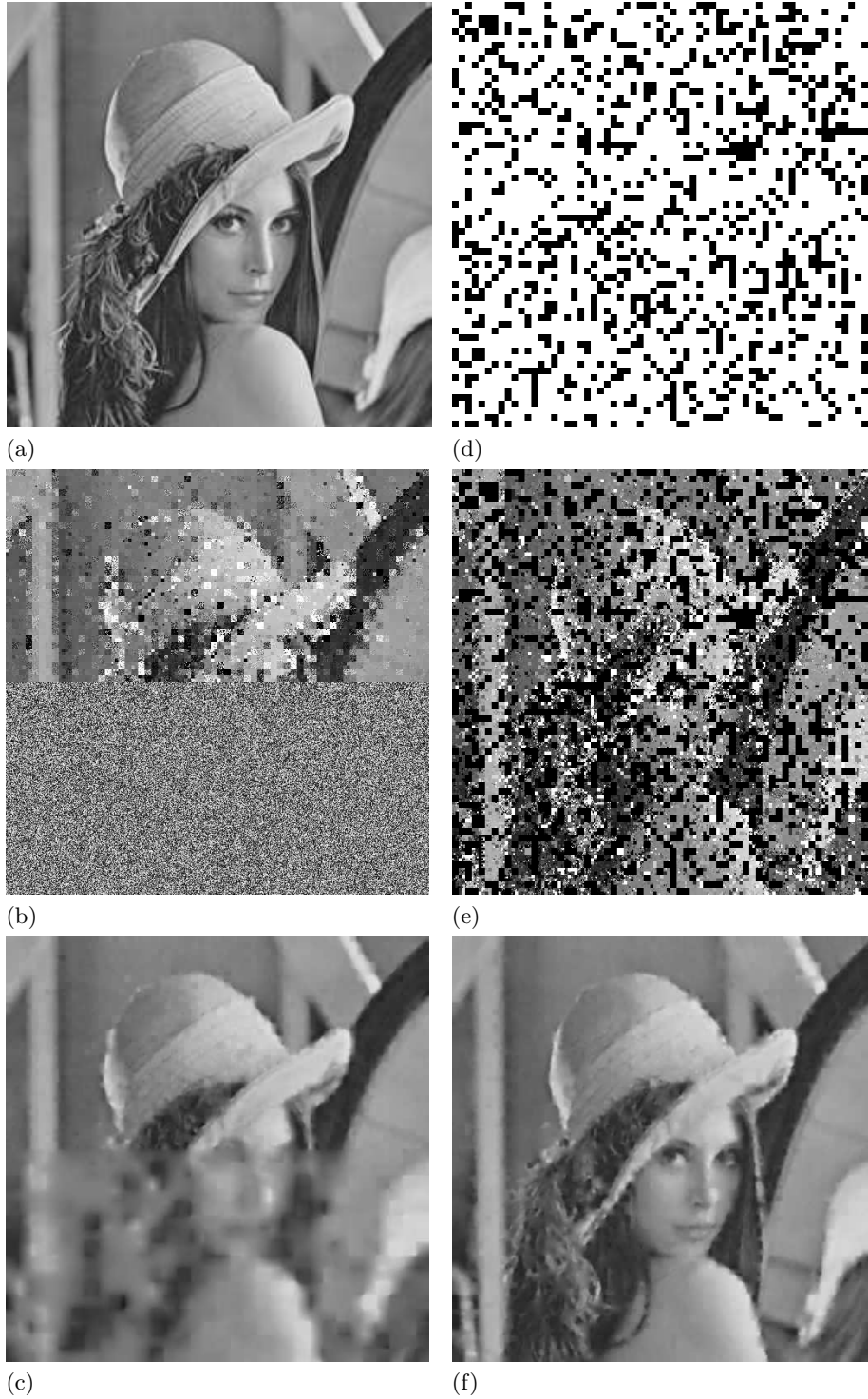


**Fig. 2.** (a) Lena original. (b) Decoded as bottom half of the fractal code is missing, random seed. (c) Proposed using POCS. (d) A quarter of the code related to the range blocks in black is missing. (e) Decoded image starting from black seed, a quarter of the fractal code is randomly missing. (f) Proposed using POCS.

in Figure 2(b). On the other hand, the POCS method alters domain and range blocks simultaneously through projections. Because of these projections, it is possible that portions of the lower part of the image are modified since some *domain blocks* used in the fractal coding procedure come from that region. The more domain blocks that lie in the region of missing fractal code (hence missing range blocks), the “fuller” the attractor that is generated by the fractal coding procedure, hence the better the approximation to the original image.

Here we come to a very important point regarding the POCS formulation of fractal coding. The usual fractal coding procedure involves mapping domain blocks onto range blocks. The POCS method of projections actually translates to a *simultaneous alteration of domain-range block pairs*. This accounts for the superior results of the POCS method in the incomplete fractal code problem.

## 5.2 Fractal image denoising

It is well known that subjecting a noisy image to a lossy compression scheme, e.g., JPEG, can produce some denoising of the image. This is also observed in the case of fractal image coding. If a noisy image is fractally coded, with little or no regard for compression, then the attractor produced by the fractal code often represents a significantly denoised version of the original image. (In fact, one can go some steps further and improve this procedure – see [9].) In such fractal image denoising algorithms, however, one performs the usual iteration procedure after the fractal code is obtained. Once again, regardless of the starting seed image, the procedure converges to the attractor of the fractal transform defined by the code. However, the POCS-based reconstruction algorithm explained in this paper can provide added flexibility. For example, if we choose the input noisy image as the starting point of the iteration, it is possible that the procedure converges to a noise-free image that is closer to the original noisy image.

As discussed earlier, the solution of the POCS-based reconstruction method – the point  $X$  of Section 3 – can also depend on the starting point of the iteration if the solution space is non-unique. A larger solution space for POCS-based fractal coding can be produced if the strict similarity constraints are relaxed to inequality constraints. Furthermore, if the original noisy image is chosen as the starting point of the POCS-based iteration, the information in this image is actually used in the reconstruction process, even after it has been used to determine the fractal code which determines the similarity/inequality constraints. Based on experiments, we believe that by choosing appropriate  $\delta$  tolerance values in the constraints, one may obtain denoised images that are visually more pleasing because they are “closer” to the original image.

Figure 3 presents the result of an experiment that agrees with this claim. The original and a noisy version of a  $256 \times 256$  image of Lena are shown in Figures 3(a) and 3(b). The fractal transform of the noisy image in Figure 3(b) corresponding to  $8 \times 8$  pixel range blocks and  $16 \times 16$  pixel domain blocks was then computed. Traditional fractal decoding produces the attractor shown in Figure 3(c). In spite of its blockiness, this image looks less noisy than the one in Figure 3(b).



**Fig. 3.** (a) Lena original. (b) The noisy Image. (c) The IFS attractor of the noisy image, using  $8 \times 8$  range blocks. (d) Proposed using POCS, the starting point is the noisy image, and the same fractal transform with  $8 \times 8$  range blocks is used, with  $\delta = |r|/3$ .

Using the same fractal code as above, we then applied the following POCS-based reconstruction method. In order to enlarge the solution space we used  $\delta = |r|/3$  at every point of the image in this experiment, where  $r$  is defined in Eq. (19). Finally, the starting point of the POCS iterations was the original noisy image shown in Figure 3(b). The result of this POCS-based procedure is shown in Figure 3(d). Although no postprocessing has been employed here, the blockiness plaguing Figure 3(c) is not visible in Figure 3(d). As well, it seems that more denoising has been achieved with Figure 3(d) than with Figure 3(c).

## 6 Conclusions

In this paper, we have described a reformulation of traditional fractal image decoding in terms of the framework of projections onto convex subsets (POCS). In the case that all the constraints defined by the fractal code are applied to the problem then the solution, defined by the intersection of all constraints, is unique and corresponds to the fixed point of the contractive fractal transform. There is a difference, however, between the POCS method and the fractal coding method regarding the nature of the respective iteration procedures and the convergence toward the solution. In the POCS method, the convergence is accomplished in a set-theoretic framework. The projections associated with POCS method involve simultaneous alteration of domain-range block pairs, unlike the case of fractal coding in which domain blocks are mapped onto range blocks, which may be viewed as a “greedy process.”

The principal advantage of the POCS framework is that it provides the flexibility to incorporate constraints and possibly additional knowledge about the reconstructed image. In this framework, it is also possible to replace the strict equality constraints associated with traditional fractal coding with inequalities that allow similarities to within some designated threshold. The latter represent more feasible and realistic conditions encountered in the real world. And, in this way, the set of feasible solutions is extended.

A POCS-based approach also provides the opportunity of solving underdetermined inverse problems in fractal coding as we have shown for the case of the incomplete fractal code problem.

Since the POCS framework allows fractal coding to be employed along with additional knowledge about the image/signal, some potential applications for future consideration include, but are not limited to, the elimination of postprocessing in fractal decoding using POCS-based reconstruction and fractal coding with overlapping domain and range pools.

Finally, recall that if all similarity constraints defined by the fractal code are applied strictly, then the solution is unique, namely, the fixed point of the associated fractal transform operator. If additional constraints are applied in a POCS-based framework, then the entire set of constraints may be inconsistent, i.e., there is no “solution” that satisfies all constraints. In this interesting situation, one may need to employ the more recent POCS formulations for inconsistent feasibility problems as studied by P. Combettes [5].

## Acknowledgements

This research was supported in part by the Natural Sciences and Engineering Research Council of Canada (NSERC) in the form of a Discovery Grant (ERV) which is hereby gratefully acknowledged.

## References

1. M.F. Barnsley, *Fractals Everywhere*, Academic Press, New York, 1988.
2. M.F. Barnsley, V. Ervin, D. Hardin and J. Lancaster, Solution of an inverse problem for fractals and other sets, *Proc. Nat. Acad. Sci. USA* **83**, 1975-1977, 1985.
3. M.F. Barnsley and L.P. Hurd, *Fractal Image Compression*, A.K. Peters, Wellesley, Mass., 1993.
4. L. M. Bregman, The method of successive projection for finding a common point of convex sets, *Soviet Math. Dokl.*, vol. 6, pp. 688-692, May 1965.
5. P. L. Combettes, *Inconsistent signal feasibility problems: Least-squares solutions in a product space*, *IEEE Transactions on Signal Processing*, vol. 42, no. 11, pp. 2955-2966, November 1994.
6. M. Ebrahimi and E.R. Vrscay, *Generalized fractal image coding using projections onto convex sets*, (preprint).
7. Y. Fisher, *Fractal Image Compression, Theory and Application*, Springer Verlag, New York, 1995.
8. B. Forte and E.R. Vrscay, Theory of generalized fractal transforms, in *Fractal Image Encoding and Analysis*, Y. Fisher, Ed., NATO ASI Series F 159, Springer Verlag, New York, 1998.
9. M. Ghazel, G. Freeman and E.R. Vrscay, *Fractal image denoising*, *IEEE Transactions on Image Processing* **12**, no. 12, 1560-1578, 2003.
10. L.G. Gubin, B.T. Polyak and E.T. Raik, *The Method of Projections for finding the Common point of Convex Sets*, *USSR Comput. Math. and Phys.*, vol. 7, no. 6, pp. 1-24, 1967.
11. N. Lu, *Fractal Imaging*, Academic Press, NY, 1997.
12. H. Puh and P. L. Combettes, *Operator Theoretic Image Coding*, Proceedings of the IEEE International Conference on Acoustics, Speech, and Signal Processing, vol. 4, pp. 1863-1866. Atlanta, GA, 1996.
13. H. Puh, *Set Theoretic Image Coding*, Ph.D. Thesis, Courant Institute, NY, 1996.
14. M.K. Ozkan, A.M. Tekalp, and M.I. Sezan, *POCS-based Restoration of Space-Varying Blurred Images*, *IEEE Transactions on Image Processing*, Volume 3, Issue 4, Page(s):450-454, July 1994.
15. D. Youla and H. Webb, *Image restoration by the method of convex projections: Part 1-Theory*, *IEEE Transactions on Medical Imaging*, vol. MI-1, no. 2, pp. 81-94, October 1982.